Received: June 17, 2024. Revised: July 26, 2024.

International Journal of
Intelligent Engineering & Systems

http://www.inass.org/

Improving the Backhaul link of the 5G Cellular Wireless Networks Using a Triple Hybrid System

Jaafar A. Aldhaibani[1]* **Ali Al-Shuwaili[1]** **Rashid Ali Fayadh[2]**

[1]*College of Engineering, University of Information Technology and Communications, Baghdad, Iraq*
[2]*Department of Electrical Engineering Techniques,*
Electrical Engineering Technical College, Middle Technical University, Baghdad, Iraq
* Corresponding author's Email: dr.jaafaraldhaibani@uoitc.edu.iq

Abstract: The recent and tremendous rise in the number of mobile users demands a parallel increase in the capacity of wireless networks required to achieve higher data rates, lower latency transmissions, and improved service quality. The latter is influenced highly by frequent interruption of wireless service for users at the edge of the cell due to the longer distance from the base station. To overcome this problem and in the meantime improve the capacity of the bottleneck backhaul in dense heterogeneous networks like 5G/6G systems especially in the cell edge regions, a hybrid solution that combines Radio Frequency (RF), Free Space Optics (FSO), and Optical Fiber (OF) links for backhaul transmission is proposed in this paper. In addition, a Backhaul Selection Algorithm (BSA) is suggested to choose the optimum link according to the outage probability analyses. This algorithm not only selects the link with the highest quality but also minimizing power consumption, thereby guaranteeing a consistently high-quality connection without interruptions of services. Using theoretical analyses and thorough simulations, the performance of the hybrid RF/FSO-OF system is evaluated and also compared to the existing state-of-the-art techniques showing the advantages of exploiting the inherited synergies of the proposal along with the selection algorithm. The numerical results reveal that the proposed system brings a considerable reduction in power consumption compared to FSO- and RF-only systems reflecting its superiority under different atmospheric channel conditions. For instance, at SNR threshold of 10 dB, the proposed system required SNR of 20, 25 and 33 dB, respectively, for weak, moderate, and strong atmospheric turbulence conditions in order to reach the outage probability of 10^{-6}.

Keywords: Free space optics, Hybrid wireless dystem, Optical fiber communication, 5G system, Radio frequency transmission, Backhaul.

1. Introduction

The advent of the new generations in the mobile communications entails tremendous increase in capacity to meet the increasing demands for higher data rates, ultra-low transmission latency as well as excellent network quality. For instance, 5G/6G transition to Heterogeneous Networks (HetNets) requires 1000-fold increase in data rates and 100-fold rise in linked wireless devices compared with what we have nowadays [1] . In order to match changing needs, future networks need to support high user level data rate, high energy efficiency level, and low latency [2]. However, in HetNets, backhaul links is used to provide connection between different tiers in the network. Since the backhaul is well understood to be often the bottleneck in such dense network deployment, 5G and beyond communication systems will be unable to support the networks by building high-speed access layers due to backhaul limitation [3].

As an alternative to the conventional radio frequency transmission, the Free Space Optics (FSO) communication utilizes the light instead of radio waves [2]. Nowadays, FSO communication has emerged as reliable candidate for a number of applications that require a lot of bandwidth. This is mainly due to the highest engine of the capacity and the unlicensed spectrum band which makes it a very suitable candidate for the implementation of cost- and energy-efficient 5G systems which can address the capacity concern of backhaul links [4].

Implementation of such FSO systems also introduces several challenges primarily the turbulence of the atmosphere which impact the propagated light [5]. Another major problem, that causes block in 5G/6G cellular networks, is the range or coverage outside the first and second main Base Station (BS). To solve this problem, a small cell networks, including Free Space Cells (FSCs), is introduced which are short-range and operate only at the cell edge. The resulting efficiency of the overall system is improved, and more mobile users can be supported [6].

The deployment of 5G networks extends the support to include a billions of connected devices such as household appliances and health monitoring equipment [7] which usually run resource-hungry mobile applications. As a result, challenges arise in the RF links, especially the bottleneck within the backhaul network at the cell boundary regions. This bottleneck is well understood to be limitations on the core network capacity to efficiently support these connected devices [8]. The main goal of introducing the FSO technology is to provide a reliable and strong backhaul link to facilitate 5G mobile cellular networks. This technology ensures secure communication, high speed, and swift data exchanges due to the large spectrum utilization and narrow laser beam [9-11]. FSO- based system implementation is essential in providing high data rates over short paths. Nevertheless, as 5G mobile applications require constant and high data transmission, its therefore imperative for FSO-based link to adapt to the changing situation of the cellular network [10, 11]. As shown in Fig. 1, and due to the absence of interference between FSO and RF technologies, the FSO technology has been chosen to enhance and support current of RF systems. Such hybrid system is applicable in many commercial scenarios like personal airplane entertainment systems to prevent any disruption to RF-delicate

Figure. 1 FSO and RF backhaul links scenarios [16]

navigation and avionics electronic devices [12]. The considered dual-band system involves choosing a hybrid RF/FSO link rather than relying solely on a standalone FSO link [13, 14]. The Mixture of FSO/RF link operates through a parallel integration of RF and FSO links. FSO link takes precedence as the primary transmission channel for data transfer, while the dedicated RF link remains on standby [15].

However, the hybrid RF/FSO systems with its enhanced backhaul connection comes with the drawback of inefficient use of RF resources.

Conversely, cognitive radio technology is recognized for its ability to optimize RF resource utilization. The integration of both technologies results in the creation of a cognitive hybrid RF/FSO system providing maximum efficiency and resource utilization [1].

Notwithstanding its benefits, FSO technology faces obstacles such as fading caused by atmospheric turbulence and channel environments. These challenges restrict FSO transmissions to short distances [17]. To extend coverage and enhance the dependability of FSO links for 5G systems, small cell stations play a crucial role in reducing the recurring interruptions in mobile services at the cell boundaries area [18].

In contrast to radio frequency transmission, the FSO communication spectrum functions without a license meaning that government delegation is not required during the installation procedure [19]. Furthermore, different encoding strategies can be used in FSO systems to lessen the impact of air turbulence [8, 9]. Since both FSO and RF systems have unique benefits to improve the dependability of backhaul lines between FSC combining FSO technology with an RF link system to create a hybrid RF/FSO communication system is one possible solution, to provide reliable communication links as shown in Fig.1 [20].

In this paper, based on the above, the RF and FSO links are integrated into one hybrid system along with wired Optical Fiber (OF) segment to provide a reliable backhaul connection capable of supporting high capacities for users and without interruption of wireless services at the cell edges. Moreover, a Backhaul Selection Algorithm (BSA) is suggested to choose the optimum link according to the outage probability analyses and received signals strength. This algorithm not only selects the link with the highest quality, but also ensures to minimize power consumption, thereby guaranteeing a consistently high-quality connection without interruptions of services.

The rest of this paper is organized as follows. Review of some recent literature is provided in

Section 2. Section 3 presents the system model with the required formulations for both RF and FSO. The proposed BSA algorithm is presented in Section 4. Section 5 is dedicated to numerical results while concluding remarks are summarized in Section 6.

2. Literature review

A hybrid transmission system that combines RF and FSO links has been proposed to counteract the impact of atmospheric conditions on the efficiency of FSO communication technology and improve the reliability and accessibility of optical communications connections. Thus, to improve performance capabilities, academics have become increasingly interested in mixed linkages in recent years. For instance, researchers in [18] developed a two-hop hybrid FSO/RF communication system that links users inside buildings to the base station by using channel status information. Hard-switching between RF and FSO links was examined by [21]. They postulate that atmospheric turbulence causes Gamma-Gamma fading at the FSO link. Only one of the links can be used at any given moment. An array of backhauling technologies, including optical fiber, FSO, RF, and their hybrid combinations have been considered in [22]. To maximize both algebraic connectedness and robustness, an iterative solution comprising two effective strategies was developed in this study. A hybrid FSO/RF communication system was suggested in [23] to guarantee dependable communication, especially when transceivers are misaligned. Two transmission media are included in this model, so the FSO and RF channels run parallel to each another. Relay switches play a crucial role in the system by seamlessly switching from the main FSO link to the RF link when bad weather interferes with transmission [14]. The usefulness of digital modulation for last-mile communication systems was examined in [24] when data transmission over hybrid fiber optic and free space optic (FO-FSO) channels were conducted.

The research evaluated the variety of digital modulation methods implemented on FSO-OF communication lines to maximize communication effectiveness [25] using sub-THz wireless link to take advantage of embedding FSO and OF technologies.

This work used a single-mode fiber through 500 m optical wireless transmission and 0.5 m through an RF wireless system where it is covered distances of up to 25 km efficiently.

The results of this integration showed that it is possible to successfully adjust high data rates in addition to multiple inputs and multiple outputs (MIMO) transmission capabilities by using new radio 5G sub-THz band. A mix of FSO/RF systems integrating various modulation procedures has been developed by [29, 30] in which the average channel capacity and outage probability issues are addressed in this system. Simulation results suggested that pointing errors worsen the impact of atmospheric turbulence on channel capacity. Moreover, when specific modulation techniques are employed in situations with several pointing errors and substantial turbulence, the performance of the RF–FSO system is noticeably improved.

The hybrid RF/FSO systems are employed to maximize the benefits of both technologies while minimizing their respective drawbacks. To optimize the performance and reliability of hybrid RF/FSO systems there are number of challenges and limitations that are addressed in the literature [28]. One of these challenges, is the cost of infrastructure in which the hybrid RF/FSO is deployed. A further drawback of this system is its complexity which is increased by the integration of two transmission technologies [29].

To this end, this work contributes to expand the user capacity at the cell edge regions through the utilization of hybrid RF/FSO-OF links connecting the wireless small cells, deployed at the cell boundaries, for coverage extension at these regions and hence increase in the number of served users. The performance of these links is investigated at atmospheric turbulence-induced fading channel conditions. In addition, we introduce an algorithm designed to choose the optimal link that offers the highest capacity taking into account factors such as received signal strength and outage probability.

This algorithm facilitates the combination of all links to effectively tracks the varying environmental conditions.

3. Materials and methods

The goal of the proposed model is to select the optimal link between RF, FSO, or a hybrid of RF/FSO lines to achieve the most efficient backhaul link to meet particular requirements for dependability, connectivity, and high data rate. The proposed model is shown in Fig. 2, where we suggest using an FSC as a multi-hop station for an RF/FSO system. The donor BS is positioned in the center of the cell in the suggested structure and the FSCs are placed in particular locations around the BS. We denote by the index j the j-th channel between the FSC and the User Equipment's (UEs), while i indicates the total number of users linked to a single FSC. Table 1 summarizes the notations and parameters used in the system model.

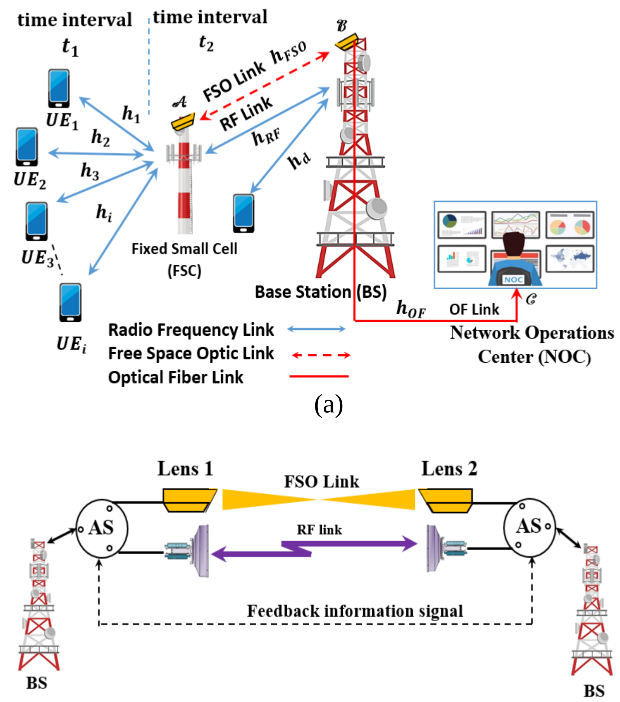

(a)

(b)

Figure. 2 Proposed model of RF/FSO – OF: (a) end-to-end with multi-hop FSC stations; (b) with Backhaul Selection Algorithm (BSA).

Table 1. System Parameters

Parameter	Description
h_i	channel coefficient of user i
h_{RF}	channel between BS and FSC
μ	coefficient of electrical to optical conversion
K_0	propagation constant of optical
I	irradiance fluctuations
γ, γ_{th}	SNR, threshold SNR
$\mathrm{P}_{out}^{Rf}, \mathrm{P}_{out}^{FSO}$	outage probability of RF and FSO link
$f_{\gamma 1}$	PDF of RF link
$K_{(a)}(0)$	2nd kind Bessel function
α, β	parameters of FSO link
σ_R^2	Rytov variance
C_n^2	turbulence intensity
C	backhaul link capacity
$G_{p,q}^{m,n}[.]$	Meijer G- function

The methodology considered in this paper is divided into three scenarios: FSO, RF, and the hybrid RF/FSO links as discussed in what follows.

3.1 Radio frequency link analysis

The received signal by a given user over the direct link h_d can be represented as [30]:

$$S_d(t) = \sqrt{P_t} h_d x(t) + \sigma(t) \tag{1}$$

In Eq. (1) above, $\sqrt{P_t}$ denotes the sent power from the BS, h_d is the channel connecting FSC and BS while $\sigma(t)$ represents the Additive White Gaussian Noise (AWGN) at the endpoint [20, 30].

This work adopts a half-duplex mode to mitigate self-interference [31, 32], in which the time intervals are divided into two segments: t_1 and t_2. As a result, the RF signal received during the initial interval $t_1$can be expressed as

$$S_{Rf}(t_1) = \sqrt{P_t} h_{\mathrm{Rf}}\, x(t_1) + \sqrt{P_f} h_{\mathrm{i}} x(t_2) + \sigma(t) \tag{2}$$

where t_1 and t_2 are the time intervals, in the context of half-duplex communication, that denote the precise times allotted for transmission and reception, respectively, to reduce self-interference. In (2), P_f is the transmitted power from FSC, h_{RF} is the channel between BS and FSC, $x(t)$ is the transmitted signal at any interval, h_{i} is the channel between FSC and UE, and the i^{th} index is the

$$P_f = \Upsilon^2 \left| \sqrt{P_t} h_{Rf} x(t_1) + \sqrt{P_{UE}} h_{\mathrm{i}} x(t_2) + \sigma(t) \right|^2 \tag{5}$$

$$\Upsilon = \sqrt{\frac{P_f}{P_t |h_{\mathrm{RF}}|^2 + P_{UE} |h_{\mathrm{i}}|^2 + \sigma(t)}} \tag{6}$$

while the received signal by the user attached with FSC is:

$$S_{UE}(t_2) = \Upsilon \sqrt{P_t} h_{Rf} x_f(t_1) + \sigma(t) \tag{7}$$

Then,

$$S_{UE}(t_2) = \Upsilon \sqrt{P_t} h_{Rf} \left(\Upsilon \sqrt{P_t} h_{\mathrm{i}} \right) + \sigma(t) \tag{8}$$

Considering the entire end-to-end communication through an RF link, the Signal-to-Noise Ratio (SNR) for the users formulated as

$$SNR = \frac{\Upsilon^2 P_t \left| h_{Rf} \right|^2 |h_{\mathrm{i}}|^2}{\left(\Upsilon^2 \left| h_{Rf} \right|^2 + 1 \right) \sigma(t)}.$$

3.2 Free space optic link analysis

To formulate the FSO signal, Subcarrier Intensity Modulation (SIM) is used, and the notation of $x_{Rf}(t_1)$ denotes the RF signal emanating from the intermediate source of FSC [33]. The retransmitted optical signal can be mathematically stated as:

$$S_{fso}(t_2) = \Upsilon(1+\mu(S_{Rf}(t_1)) \quad (9)$$

where μ represents the coefficient of electrical to optical conversion that influences the process at the destination Lens 2 (see Fig. 2 (b)). The received signal, in this case, was reads

$$S_{fso}(t_2) = K_0 I\{\Upsilon(1+\mu(S_{Rf}(t_1))\} + \sigma(t) \quad (10)$$

where K_0 denotes the propagation constant of optical and I signifies irradiance fluctuations resulting from fading induced by atmospheric turbulence [1, 27]. The signal that is received at the destination can be reformulated, by filtering the cumulative distribution function (CDF) component, as

$$S_{fso}(t_2) = I\Upsilon\mu(S_{Rf}(t_1) + \sigma(t) \quad (11)$$

By substituting with Eq. (2) get:

$$S_{opt}(t_2) = I\{\Upsilon(1+\mu(\sqrt{P_t}h_i\, x(t_1) + \sqrt{P_{Rf}}h_{Rf}x(t_2) + \sigma(t))\} \quad (12)$$

The AWGN term $\sigma(t)$ represents Normally-distributed noise the zero mean and variance $N_o/2$ [24].

Thus, the end-to-end SNR of hybrid links of h_{Rf} and h_{FSO}. These quantities can written as [34]:

$$\gamma_{fso} = \frac{I^2\mu^2\Upsilon^2|h_i|^2P_t}{I^2\mu^2\Upsilon^2\sigma(t)} \quad (13)$$

$$= \frac{\frac{|h_i|^2P_tI^2\mu^2}{\sigma(t)}}{\frac{I^2\mu^2}{\sigma(t)} + \frac{1}{\Upsilon^2\sigma(t)}} \quad (14)$$

To simplify the formulations in (13) and (14), let the $M = 1/\Upsilon^2\sigma(t)$ and $\gamma_1 = |h_i|^2P_t/\sigma(t)$ and $\gamma_2 = I^2\mu^2/\sigma(t)$. Here, γ_1 symbolizes SNR of the initial hop from the BS to the FSC, while γ_2 represents the SNR of the second hop from the FSC to users via h_{FSO} exclusively. Thus, we can express Eq. (14) as follows: [34, 35]

$$\gamma_{fso} = \frac{\gamma_1\gamma_2}{\gamma_2+M}. \quad (15)$$

The SNR is determined by various factors including the quality of service (QoS), the path between the transmitter and receiver d and channel noise. The channel coefficient can be expressed as [11].

$$|h|^2 = \eta(d)^{-a}, \quad (16)$$

where η represents a parameter associated with the channel characteristics and a is the path loss exponent [36].

We assume that fading has Probability Density Function (PDF) that is Rayleigh distributed. The direct link between the BS and FSCs follows a Rayleigh PDF. If the SNR drops below a designated threshold γ_{th}, it is then considered an outage. Under such condition, the PDF of the RF link is then has the form [14].

$$f_{\gamma1}(\gamma_1) = \frac{1}{\gamma_{th,Rf}}e^{-\gamma_1/\gamma_{th,Rf}}. \quad (17)$$

In (17), $\gamma_{th,Rf}$ represents the threshold SNR for the RF link. Based on [37], the outage probability can be approximated by evaluating CDF of the RF link, obtained by integrating Eq. (17).

$$\mathrm{P}_{out}^{Rf} = \int_0^{\gamma_{th,Rf}} f_{\gamma1}(\gamma_1) = 1 - e^{-\gamma_1/\gamma_{th,Rf}} \quad (18)$$

In order to provide a thorough and precise analysis, the Gamma-Gamma fading model is assumed to model the effect of atmospheric turbulence on FSO connections in the proposed hybird RF/FSO-OF. Morever, it is ensuring robust and reliable performance analysis even in the presence of large fluctuations in refractive index. Thus the connection between the FSC and FSO is presumed to undergo gamma-gamma fading distribution, as outlined in the PDF represented as follows:[18, 20].

$$f_{\gamma2}(\gamma_2) = \frac{(\alpha\beta)^{(\alpha+\beta)/2}\gamma_2{}^{(\alpha+\beta)/4}}{\Gamma(\alpha)\Gamma(\beta)\overline{\gamma}_2^{(\alpha+\beta)/4}}K_{(\alpha-\beta)}\left(2\sqrt{\alpha\beta\sqrt{\frac{\gamma_2}{\overline{\gamma_2}}}}\right) \quad (19)$$

The average SNR of the FSO link, denoted as $\overline{\gamma_2}$, is calculated, where $K_{(a)}(0)$ represents the Bessel function of the second kind with an order a. The atmospheric turbulence conditions for the FSO link is characterized by the parameters α, and β are defined in Eq. (5) and Eq. (6) as provided below [19, 20] :

$$\alpha \cong exp\left[\frac{0.49\sigma_R^2}{(1+0.11\sigma_R^{\frac{12}{5}})^{7/6}}\right] - 1 \quad (20)$$

Received: June 17, 2024. Revised: July 26, 2024.

$$\beta \cong exp\left[\frac{0.51\sigma_R^2}{(1+0.69\sigma_R^{\frac{12}{5}})^{7/6}}\right]-1 \quad (21)$$

where σ_R^2 is Rytov variance as mentioned in Eq. (21) and defined in Eq. (7) of [38].

$$\sigma_R^2 = 1.23(\frac{2\pi}{\lambda})^{7/8}C_n^2\mathcal{L}^{11/6} \quad (22)$$

with C_n^2 representing the altitude-dependent turbulence intensity, and it varies from 10^{-17} to 10^{-13} $\mathrm{m}^{-2/3}$ according to the circumstances of atmospheric turbulence, $\mathcal{L}$ is the distance of the optical link [37]. To elaborate more on the CDF in (18), the Gamma - Gamma distribution of FSO link can be expressed differently as:

$$\mathrm{P}_{out}^{fso} = \frac{(\alpha\beta)^{(\alpha+\beta)/2}\gamma_2{}^{(\alpha+\beta)/4}}{\Gamma(\alpha)\Gamma(\beta)\bar{\gamma}_2^{(\alpha+\beta)/4}}G_{1,3}^{2,1}\left(\alpha\beta\sqrt{\frac{\gamma_2}{\bar{\gamma}_2}}\Bigg|\begin{matrix}1-\frac{\alpha/\beta}{2}\\ \frac{\alpha-\beta}{2},\frac{\beta-\alpha}{2},\frac{\alpha+\beta}{2}\end{matrix}\right) \quad (23)$$

where the $G_{p,q}^{m,n}[.]$ is the Meijer G- function as stated by [23, 37, 38]. So, the outage probability of both RF and FSO links stated in (17) and (22), respectively, can be reformulated as:

$$\mathrm{P}_{\mathrm{out}}^{\mathrm{Rf/fso}} = \frac{(\alpha\beta)^{(\alpha+\beta)/2}\gamma_2{}^{(\alpha+\beta)/4}}{\Gamma(\alpha)\Gamma(\beta)\bar{\gamma}_2^{(\alpha+\beta)/4}}\mathrm{G}_{1,3}^{2,1}\left(\alpha\beta\sqrt{\frac{\gamma_2}{\bar{\gamma}_2}}\Bigg|\begin{matrix}1-\frac{\alpha/\beta}{2}\\ \frac{\alpha-\beta}{2},\frac{\beta-\alpha}{2},\frac{\alpha+\beta}{2}\end{matrix}\right)\left(1-e^{-\gamma_1/\gamma_{\mathrm{th,Rf}}}\right) \quad (24)$$

The channel capacity $\bar{\mathrm{C}}$ of the hybrid RF/FSO backhaul link can be mathematically stated as [39].

$$\bar{\mathrm{C}} = C^{fso}(\bar{\gamma}_2) + \mathrm{P}_{out}^{fso}(\bar{\gamma}_2)C^{Rf}(\gamma_{th,Rf}) \quad (25)$$

$\mathrm{P}_{out}^{fso}(\bar{\gamma}_2)$ is given in Eq. (23), $C^{fso}(\bar{\gamma}_2)$ and $C^{Rf}(\gamma_{th,Rf})$ are the capacity of channel via RF and FSO links, respectively. In reference to Eq. (16) and Eq. (18), and if both links are in operation, we have:

$$C^{fso}(\bar{\gamma}_2) = \int_{\gamma_{th}}^{\infty} BW^{fso}\cdot log_2(1+\gamma)f_{\gamma 2}(\gamma_2)d\gamma \quad (26)$$

$$C^{Rf}(\gamma_{th,Rf}) = \int_{\gamma_{th}}^{\infty} BW^{RF}\cdot log_2(1+\gamma)f_{\gamma 1}(\gamma_1)d\gamma \quad (27)$$

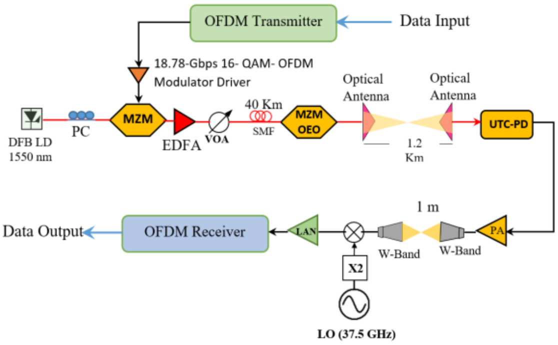

Figure. 3 Framework for Integrated Fiber and Free-Space Optical Communication Systems

where the BW^{Rf} and BW^{fso} are the bandwidths of the RF and FSO links respectively.

$$\mathrm{C}(\gamma_{th}) = \int_{\gamma_{th}}^{\infty} log_2(1+\gamma) \quad (28)$$

3.3 First-order headings

In this section, taking advantage of the proposed hybrid system discussed previously, we augment the proposed design with an integrated FSO-OF communication system, as demonstrated in Fig. (3). Recall that in Fig. 2 (a).

This design presents a wired/wireless link between point B and point C which employs multi-carrier modulation to mitigate dispersion-induced RF fading and also optical beating carried on by multiple-carrier signal interference.

The system is examined using multi-carrier frequencies of 100 GHz and 150 GHz to simulate different scenarios. This leads to the realization of a hybrid OF-FSO system operating at millimeter-wave (MMW) and sub-terahertz (sub-THz) frequencies. At each MMW/sub-THz frequency, an 18.78-Gbps 16-quadrature amplitude modulation (QAM) with orthogonal frequency-division multiplexing (OFDM) signal is transmitted [40]. In the proposed setup, a 40 km Single-Mode Fiber (SMF) transmission for the OF link along with a 1.2 km wireless FSO connection are utilized for this system. The optical carrier is generated by a distributed laser diode which operates at the wavelength of 1550 nm. This carrier is modulated using a Mach-Zehnder modulator (MZM). The MZM is driven by the 18.78 Gbps 16-QAM-OFDM signal from the OFDM transmitter after passing through the modulator driver.

4. The proposed backhaul selection algorithm (BSA)

In this section, the Backhaul Selection Algorithm (BSA) is presented that select the optimal backhaul

Received: June 17, 2024. Revised: July 26, 2024.

connection between hybrid RF and FSO links. This method operates by assessing the overall performance according to end-to-end SNR of the link and probability of outage for RF and FSO transmissions (c.f. (18), (23), and (24)). BSA doesn't require any extra channel state information (CSI) at the transceiver or feedback data. Moreover, this algorithm guarantees the data transmission rates are identical for the three links simultaneously as opposed to transmission rate via a single connection. If the selected RF connection does not satisfy the designated outage threshold, an FSO link or a mix of FSO and RF links may be used in place.

As illustrated in Fig. 4, this algorithm involves a process that evaluates the outage probability which, in turns, entails the computation of various parameters such as link quality, signal strength and SNR.

This process is then repeated for finding the outage probability over the three links, i.e., RF, FSO, and hybrid RF/FSO to determine the optimal backhaul link under different conditions. The complete steps are depicted in the flowchart in Fig. 4. The operation of BSA along with the hybrid RF/FSO brings two main advantages: first, it ensures seamless wireless service for users at the cell edge region and hence maintain reliability and service quality of the connection. Second, it can decrease overall power consumption due to utilization of the more power-efficient FSO links and reducing the need for power-intensive RF links, thus contributing to lower power consumption. The length of time the FSO system runs determines how much power is saved.

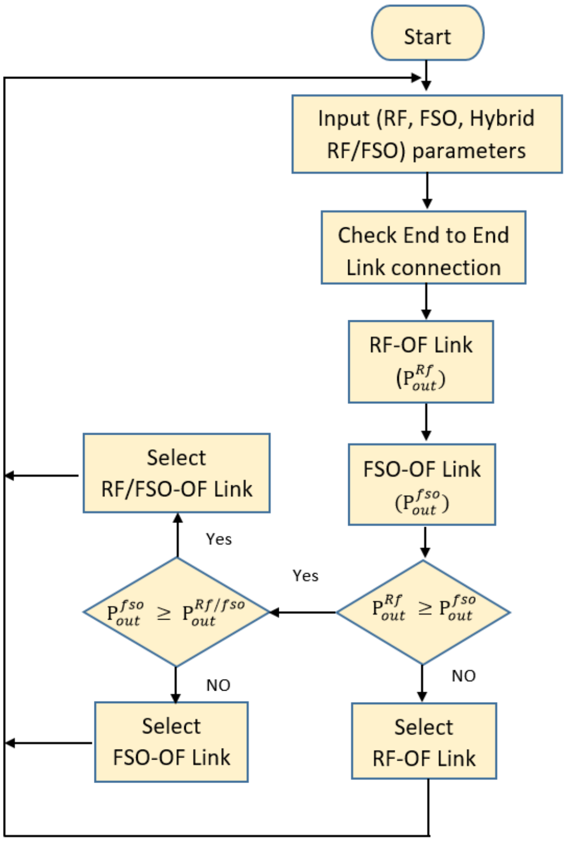

Figure. 4 The Suggested Backhaul Selection Algorithm (BSA) to elect the optimal backhaul link.

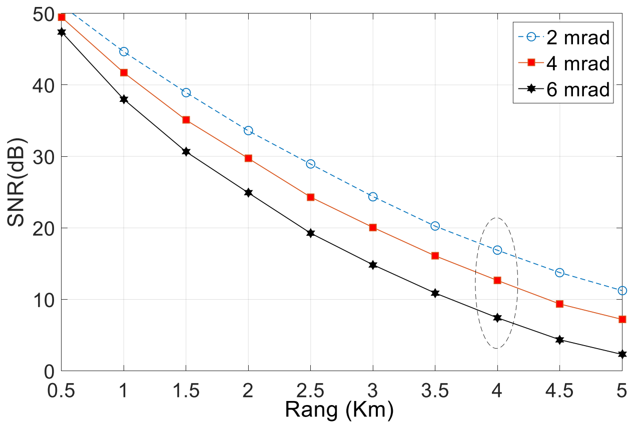

Figure. 5 SNR in relation to link range under different beam divergence situations.

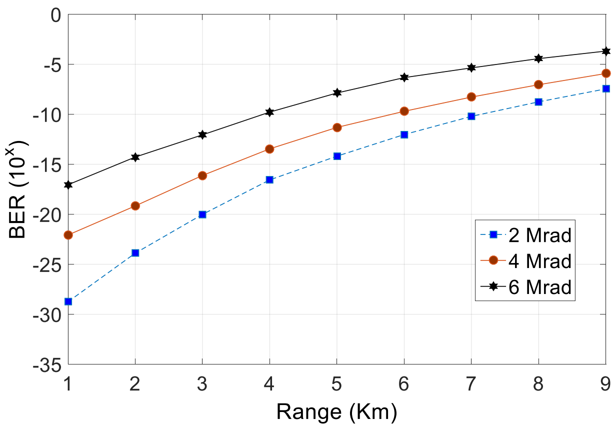

Figure. 6 BER in relation to link range under different beam divergence situations.

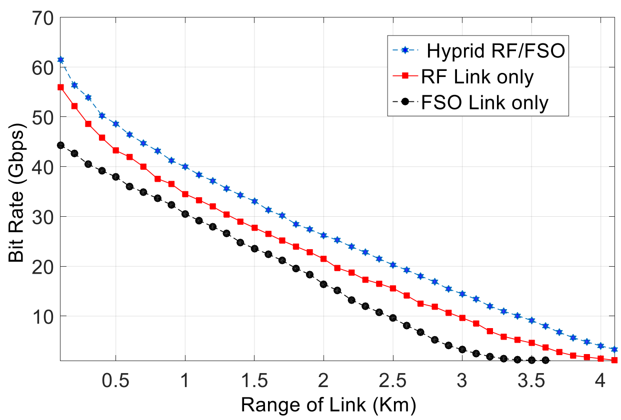

Figure. 7 The relationship between the proposed RF/F

 DOI: 10.22266/ijies2024.1031.54

Received: June 17, 2024. Revised: July 26, 2024.

Table 2. Link specifications for the suggested FSO system [43,44]

Parameters	Value
Laser power	10 dBm
Wavelength	1550 nm
Data rate	10 GHz
Transmitter Aperture diameter	5 cm
Beam divergence	2 – 6 mrad
Receiver Aperture diameter	20 cm
Photodetector type	APD
Responsivity of APD	1 A/W
Dark Current	10 nA
Link distance $\mathcal{L}$	1200m
Weak Turbulence C_n^2	$8.4\ x\ 10^{-15}\ m^{-2/3}$
Moderate Turbulence C_n^2	$1.7\ x\ 10^{-14}\ m^{-2/3}$
Strong Turbulence C_n^2	$5\ x\ 10^{-14}\ m^{-2/3}$

5. Results and discussion

In this section, we provide some numerical results to validate and assess the performance of the proposed hybrid scheme and the BSA algorithm. The power transmitted through FSO link is assumed to stand at 320 milliwatts, while for the RF link, it is set at 16 milliwatts. To simulate the effect of the atmospheric turbulence conditions, the typical values were employed as outlined in [26, 44], with β equals to 1.342 and α equals to 2.064. Likewise, for the Gamma-Gamma distribution pertaining to strong atmospheric turbulence, we opted for standard parameters (α = 2.064, β = 1.342) [42]. The simulation parameters for the proposed system are summarized in Table 2.

Fig. 5 plots the achievable SNR as a function of the range, or distance, between FSC and BS. The figure shows the SNR performance across various link ranges within the designed FSO system. The SNR experiences notable changes as the beam divergence of the FSO system is adjusted. With reduced beam divergence, the SNR levels of the FSO system are deemed adequate, while an escalation in beam divergence correlates with a decline in SNR values within the FSO system. For instance, at a distance of 4 km, the SNR values for the designed FSO system are 16.79 dB, 12.7 dB, and 7.6 dB, aligned with beam divergence settings of 2 mrad, 4 mrad, and 6 mrad, respectively.

Fig. 6 depicts the performance of the designed FSO system in terms of BER across various beam divergence profiles. An observation reveals a degradation in BER performance with an increase in transmission distance. Furthermore, it is notable that BER performance deteriorates as the beam divergence expands from 2 to 6 mrad as shown in the figure.

The FSO communication link offers a notable advantage in terms of its unrestricted bandwidth. However, when the optical line-of-sight signal traverses through the atmospheric channel, it encounters challenges stemming from the increased distance between the transmitter and receiver.

This results in attenuation, which includes absorption and scattering, as well as the presence of scintillation effects. The primary concern in 5G/6G cellular networks revolves around the incessant need for high data rates. This is predominantly due to the fact that RF backhaul links are constrained by limited bandwidth, leading to communication bottlenecks arising from bandwidth congestion. As the link distance increases, the visibility of the channel diminishes, resulting in higher optical signal loss as it traverses through the channel. Consequently, this leads to decrease in the received optical power on the Avalanche Photodiode (APD) window of an optical receiver resulting in a reduction in the bit rate.

To this end, using parameters from Table 2, we examine in Fig. 7 the bit rate of the proposed system with BSA under three considered scenarios: conventional RF link only, FSO only, and hybrid RF/FSO. The results unequivocally show that the combined RF/FSO system surpasses the performance of RF and FSO individually in terms of data rate. This means the 5G and beyond network expansion is made possible with scalable and adaptable solutions offered by a hybrid RF/FSO-OF system. The solution can also be regarded as a drastic fix for inadequate coverage at the cell boundaries.

Fig. 8 illustrates the correlation between BER and transmitted power for the suggested hybrid RF/FSO scheme across different weather conditions. The RF fading parameter is set to $m = 2$ and receiver aperture diameters set at $D = 10$ cm [45–47]. In this figure, it is evident that the BER is susceptible to

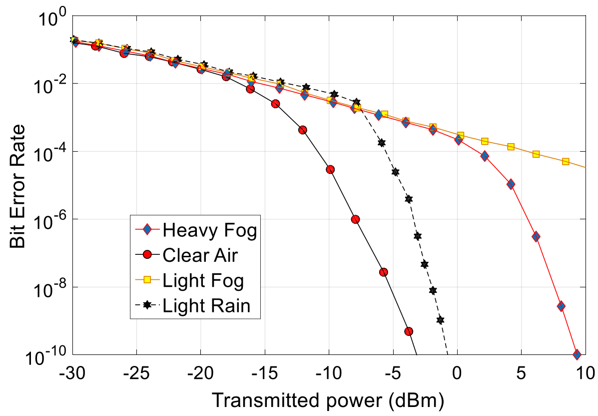

Figure. 8 The BER verses variation of transmitted power for the hybrid RF/FSO under different weather conditions.

Received: June 17, 2024. Revised: July 26, 2024.

fluctuations influenced by various weather conditions. In specific, light fog exerts the most significant impact, whereas clean air demonstrates the least effect. As transmitted powers increase sufficiently, the BERs experience rapid declines. The transmitted power associated with the turning, or knee, point also tends to be higher in weather conditions characterized by greater light attenuation. The reason behind this phenomenon is that, at low transmitted power levels, the primary factor influencing the BER is the attenuation of light intensity. Consequently, a modest increase in transmitted power leads to a consistent decrease in the BER curve. However, as the transmitted power reaches higher levels, the main factor impacting the BER shifts is turbulence. Hence a substantial increase in transmitted power will result in a sharp decline in the BER. These findings assert that while the BER of the hybrid direct link is notably influenced by both the FSO and RF links, enhancements in either link can notably enhance the BER performance of the hybrid direct link as shown in Fig. 8. As a result, the suggested system keeps up its performance without requiring adaptive processing or appreciably higher power usage. This is especially crucial for small cells of FSC whose daily strength of air turbulence fluctuates often. Changing system parameters all the time in certain situations might be counterproductive and can cause performance degradation. On the other hand, the suggested solution maintains performance without requiring extra processing or power.

Fig. 9 illustrates the outage probability of the proposed hybrid RF/FSO system in reference to the outage of the two benchmarks, namely RF outage in (18) and FSO outage in (23) which are all dependent on the average end-to-end SNR. The results demonstrate that the proposed RF/FSO system surpasses other cases in terms of reliability and the adoption of the proposed BSA notably improves the performance of the proposed system even further.

Also, the outcomes of the outage analysis revealed the superiority and resilience of the hybrid FSO/RF system in contrast to the FSO-only system across a range of turbulence scenarios (more on this point in Fig. 11). The outcomes unequivocally showed that, under all turbulence situations the suggested hybrid RF/FSO system efficiently takes advantage of the complimentary characteristics of the FSO and RF channels, as evidenced in Fig. 9.

In the hybrid RF/FSO connection, having unregulated bandwidth stands out as a key advantage for achieving higher capacity of the backhaul link which relies heavily on the achievable SNR quality. Fig. 10 illustrates the correlation between the link

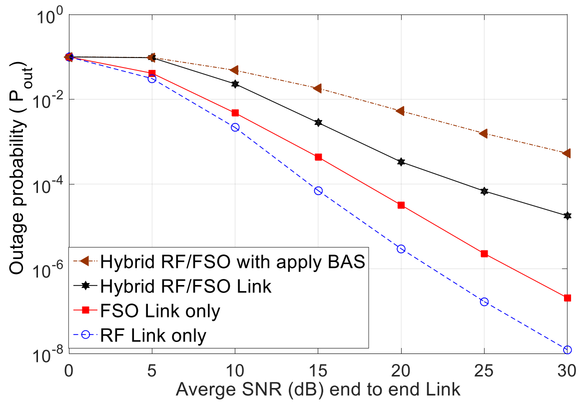

Figure. 9 The relationship of outage probability vs SNR for three scenarios RF/FSO, FSO, and RF links before and after applying BSA.

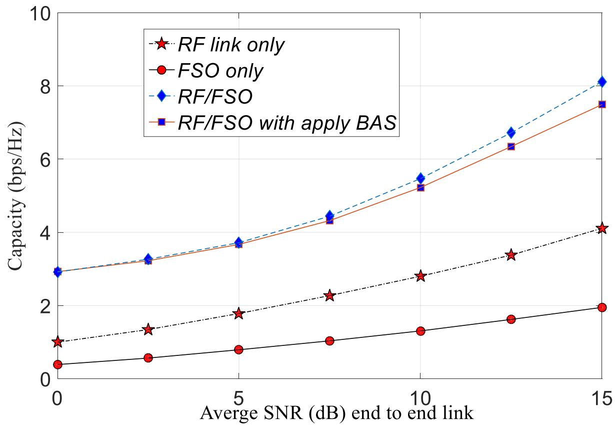

Figure. 10 The relationship between the link capacity and the average end-to-end SNR for RF/FSO, FSO, and RF links before and after applying BSA.

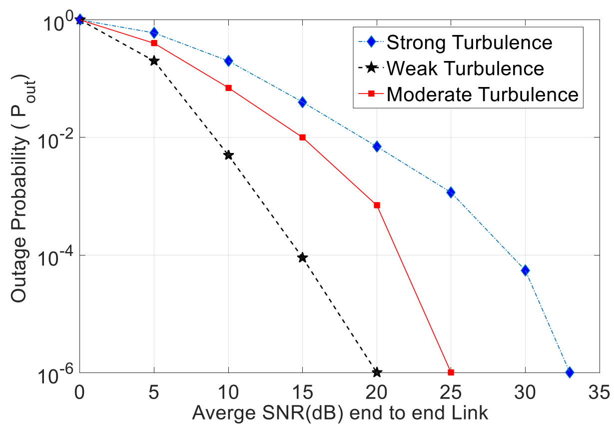

Figure. 11 The relationship of outage probability vs SNR of the proposed RF/FSO-OF system under different atmospheric turbulence conditions.

Table 3. Performance comparison

Ref.	SNR (dB)	C (bps/Hz)	P_{out}
[22]	15	3	$16x10^{-2}$
[23]	15	6.5	$14x10^{-2}$
Proposal	15	8	$16x10^{-4}$

capacity and the average end-to-end SNR for the four schemes considered in Fig. 9, namely hybrid RF/FSO link, FSO link, RF link and Hybrid RF/FSO after utilization of the proposed BSA algorithm. Fig. 10 demonstrates that as the SNR value rises, there is a corresponding increase in the link capacity. Notably, after applying the proposed BSA, the link capacity of the hybrid RF/FSO system far exceeds the capacity of both standalone FSO and RF links. The figure also shows the benefits of the proposed system that use of both RF and FSO advantages to guarantee the high availability of backhaul link and dependability for 5G applications, such as enhanced Mobile Broadband (eMBB), disaster recovery and large-scale festivals and celebrations that need for constant connections with huge capacities are supported by this system's high capacity and dependability. Notably, our results which are demonstrated in Figures 9 and 10 show that the proposed hybrid RF/FSO model performs noticeably better than existing schemes in the literature, e.g. [22, 23] in terms of link capacity and outage probability. To elaborate more on this point, we have reported numerically, in Table 3, the results of the comparison between the proposed BSA-based hybrid scheme with some schemes from the literature as shown in Table 3 below. The data from the table indicate that the performance of the proposed system is superior to other benchmark schemes in terms of link capacity and outage probability.

Finally, Fig. 11 shows the outage probability performance versus end-to-end SNR of the proposed hybrid RF/FSO-OF system under different atmospheric turbulence conditions, that is weak, moderate, and strong turbulence (using parameters defined in Table 2). The results depicted in the Fig.11 show that the system's performance decreased as atmospheric turbulence increased. For example, at SNR threshold of $\gamma_{th} = 10$ dB, the proposed system required SNR of 20, 25 and 33 dB, respectively, for weak, moderate, and strong atmospheric turbulence conditions in order to reach the outage probability of 10^{-6}.

The last result shed light on another virtue of the proposed hybrid scheme, that is the capability of the scheme to perform well even in low SNR regime. This means that practical systems can benefit from the proposal in efficiently operating low power devices like battery-powered IoT devices.

6. Conclusion

In pursuit of providing reliable and resourceful backhaul links, this paper proposes new approach to implement the hybrid RF/FSO-OF system that can support higher data rate, lower power consumption and enhanced coverage for user located at cell boundaries. We also derive new formulations for average BER and outage probability for the proposed RF/FSO-OF, as well as two special cases, i.e., RF- and FSO-only, to analyse its effectiveness under different atmospheric turbulence conditions. Using the obtained analytical expressions for the outage probability and ergodic capacity, BSA algorithm is also proposed for link optimization. This algorithm aims to select the optimal backhaul link. Numerical findings demonstrated that the mixed RF/FSO-OF backhaul link outperforms other links across various turbulence scenarios in term of bit rate and capacity at cell edge regions and achieved low values of outage probability than other links. Moreover, the mixed RF/FSO exhibits superior performance significantly enhancing conductivity and dependability compared to RF or FSO individually. The results of this work can be applied as a guideline when installing a workable RF/FSO backhaul link and also to forecast system performance, like determine the maximum achievable range within environmental variations.

Conflicts of Interest

The authors hereby provide confirmation on conflict of interest.

Author Contributions

Conceptualization, Aldhaibani and Al-Shuwaili; methodology, Aldhaibani, Al-Shuwaili and, and Fayadh; software and validation, Aldhaibani and Al-Shuwaili; formal analysis, Aldhaibani, Al-Shuwaili; resources and data curation, Aldhaibani, Al-Shuwaili and, and Fayadh; writing-original draft preparation, Aldhaibani; writing-review and editing, Aldhaibani, Al-Shuwaili, and Fayadh. All authors have recited and accepted the final manuscript.

References

[1] O. Aboelala, I. E. Lee, and G. C. Chung, "A survey of hybrid free space optics (FSO) communication networks to achieve 5G connectivity for backhauling", *Entropy*, Vol. 24, No. 11, p. 1573, 2022.

[2] M. J. Alam, M. R. Hossain, S. Azad, and R. Chugh, "An overview of LTE/LTE-A heterogeneous networks for 5G and beyond", *Transactions on Emerging Telecommunications Technologies*, p. e4806, 2023.

[3] J. Yu, H. Zhang, Y. Chen, and Y. Ruan, "Performance Analysis of Backhaul-Aware User Association in 5G Ultradense

Heterogeneous Networks", *Wireless Communications and Mobile Computing*, Vol. 2021, pp. 1-13, 2021.

[4] S. A. H. Mohsan, M. A. Khan, and H. Amjad, "Hybrid FSO/RF networks: A review of practical constraints, applications and challenges", *Optical Switching and Networking*, Vol. 47, p. 100697, 2023.

[5] H. Kashif and M. N. Khan, "Outage Probability Analysis of Free Space Communication System Using Diversity Combining Techniques", *Computers, Materials & Continua*, Vol. 73, No. 3, 2022.

[6] T. M Jamel, A. Al-Shuwaili, and B. M Mansoor, "Novelty Study of the Window Length Effects on the Adaptive Beam-forming Based-FEDS Approach", *International Journal of Computing and Digital Systems*, Vol. 9, No. 6, pp. 1221-1227, 2020.

[7] A. Al-Shuwaili, M. Dh Hassib, and T. M Jamel, "Ball's-Based Adaptive Channel Estimation Scheme Using RLS Family-Types Algorithms", *International Journal of Computing and Digital Systems*, Vol. 12, No. 1, pp. 469-477, 2022.

[8] D. Singh, R. Swaminathan, and A. T. Pham, "Multiple HAPS-based space-air-ground network with FSO communication: a performance analysis", *Applied Optics*, Vol. 63, No. 9, pp. 2362-2375, 2024.

[9] S. M. El-Garhy, A. A. M. Khalaf, M. Abaza, and M. H. Aly, "Intelligent transportation system using wireless optical communication: a comparative study", *Optical and Quantum Electronics*, Vol. 56, No. 2, p. 247, 2024.

[10] R. F. Miranda *et al.*, "A Review of Cognitive Hybrid Radio Frequency/Visible Light Communication Systems for Wireless Sensor Networks", *Sensors*, Vol. 23, No. 18, p. 7815, 2023.

[11] J. A. Aldhaibani and N. A. Al-Shareefi, "Free space optics backhaul link for small cells of 5G cellular networks", *Journal of Engineering Science and Technology*, Vol. 15, No. 3, pp. 1685-1697, 2020.

[12] M. M. Fadoul, "Modeling multi-tier heterogeneous small cell networks: rate and coverage performance", *Telecommunication Systems*, Vol. 75, No. 4, pp. 369-382, 2020.

[13] H. Lei *et al.*, "On Secure Mixed RF-FSO Systems with TAS and Imperfect CSI", *IEEE Transactions on Communications*, Vol. 68, No. 7, pp. 4461-4475, 2020.

[14] I. Trigui, S. Affes, A. M. Salhab, and M. S. Alouini, "Multi-User Mixed FSO-RF Systems with Aperture Selection under Poisson Field Interference", *IEEE Access*, Vol. 7, pp. 73764-73781, 2019.

[15] S. Nath, S. P. Singh, and S. Sengar, "Interference and noise analysis for hybrid FSO/RF-based 6G mobile backhaul", *ETRI Journal*, Vol. 44, No. 6, pp. 966-976, 2022.

[16] E. Zedini, I. S. Ansari, and M. S. Alouini, "Performance analysis of mixed Nakagami-m and gamma-gamma dual-hop FSO transmission systems", *IEEE Photonics Journal*, Vol. 7, No. 1, 2015.

[17] K. Shahiduzzaman, M. F. Haider, and B. K. Karmaker, "Terrestrial free space optical communications in Bangladesh: Transmission channel characterization", *International Journal of Electrical and Computer Engineering*, Vol. 9, No. 4, pp. 3130-3138, 2019.

[18] M. A. Amirabadi and V. T. Vakili, "Performance analysis of a novel hybrid FSO/RF communication system", *IET Optoelectronics*, Vol. 14, No. 2, pp. 66-74, 2020.

[19] E. Erdogan, I. Altunbas, N. Kabaoglu, and H. Yanikomeroglu, "A cognitive radio enabled RF/FSO communication model for aerial relay networks: Possible configurations and opportunities", *IEEE Open Journal of Vehicular Technology*, Vol. 2, pp. 45-53, 2020.

[20] J. A. Aldhaibani, Y. N. Jurn, and N. I. Abdulkhaleq, "Performance evaluation of dual backhaul links RF/FSO for small cells of 5G cellular system.", *International Journal of Electrical & Computer Engineering*, Vol. 12, No. 4, 2022.

[21] K. O. Odeyemi and P. A. Owolawi, "Partial relay selection in mixed RF/FSO dual-hop system over unified M-distributed fading channel with non-zero boresight pointing errors", *Optical and Quantum Electronics*, Vol. 51, No. 5, 2019.

[22] B. Bag, A. Das, C. Bose, and A. Chandra, "Hybrid FSO/RF-FSO systems over generalized Málaga distributed channels with pointing errors", In: *Proc. of 2019 27th European Signal Processing Conf (EUSIPCO)*, A Coruna, Spain, pp. 1-5, 2019.

[23] Y. Wu, M. Jiang, G. Li, and D. Kong, "Systematic performance analysis of hybrid FSO/RF system over generalized fading channels with pointing errors", *Photonics*, MDPI, 2022, p. 873.

[24] M. V. Kumar, V. Kumar, and R. Singh, "Investigation of PSK/QAM Modulated Hybrid Fiber Optic and Free Space Optic System Under Various Atmospheric Losses", *ASEAN*

Engineering Journal, Vol. 13, No. 1, pp. 51-57, 2023.

[25] M. Alsharari, K. Aliqab, F. Ali, and A. Armghan, "Integrated Free-Space Optics and Fiber Optic Network Performance Enhancement for Sustaining 5G High Capacity Communications", *International Journal of Optics*, Vol. 2023, 2023.

[26] T. Jiang *et al.*, "Performance improvement for mixed RF-FSO communication system by adopting hybrid subcarrier intensity modulation", *Applied Sciences*, Vol. 9, No. 18, p. 3724, 2019.

[27] M. A. Esmail, "Performance monitoring of hybrid all-optical fiber/FSO communication systems", *Applied Sciences*, Vol. 13, No. 14, p. 8477, 2023.

[28] M. Ibrahim *et al.*, "Anticipating Optical Availability in Hybrid RF/FSO Links Using RF Beacons and Deep Learning", *arXiv preprint arXiv:2405.13366*, 2024.

[29] P. S. Bithas, H. E. Nistazakis, A. Katsis, and L. Yang, "Hybrid FSO/RF Communications in Space-Air-Ground Integrated Networks: A Reduced Overhead Link Selection Policy", *Electronics*, Vol. 13, No. 4, p. 806, 2024.

[30] J. Lin, G. Wang, R. Fan, Y. Zou, T. A. Tsiftsis, and C. Tellambura, "Feature-oriented channel estimation in reconfigurable intelligent surface-assisted wireless communication systems", *IET Communications*, Vol. 14, No. 19, pp. 3458-3463, 2020.

[31] Y. Wang *et al.*, "A Full-Duplex 60 GHz Transceiver with Digital Self-Interference Cancellation", *Electronics*, Vol. 13, No. 3, p. 483, 2024.

[32] M. Madani Fadoul and C.-O. Chow, "Half-duplex and full-duplex interference mitigation in relays assisted heterogeneous network", *Plos one*, Vol. 18, No. 6, p. e0286970, 2023.

[33] H. Khalid, S. Sheikh Muhammad, H. E. Nistazakis, and G. S. Tombras, "Performance analysis of hard-switching based hybrid FSO/RF system over turbulence channels", *Computation*, Vol. 7, No. 2, pp. 1-10, 2019.

[34] H. Samimi and M. Uysal, "End-to-end performance of mixed RF/FSO transmission systems", *Journal of Optical Communications and Networking*, Vol. 5, No. 11, pp. 1139-1144, 2013.

[35] M. H. Al-mekhlafi, A. S. Ibrahim, Y. A. Fahmy, and M. M. Khairy, "Resilient hybrid optical-RF backhauling for tiered networks", *Physical Communication*, Vol. 36, p. 100814, 2019.

[36] X. J. Zhang and Y. Gong, "A simple amplify-and-forward relaying scheme based on clipping and forwarding for dual-hop transmissions", *Journal of Communications*, Vol. 5, No. 4, pp. 348-353, 2010.

[37] H. E. Nistazakis, T. A. Tsiftsis, and G. S. Tombras, "Performance analysis of free-space optical communication systems over atmospheric turbulence channels", *IET Communications*, Vol. 3, No. 8, pp. 1402-1409, 2009.

[38] M. I. Aal-Nouman, O. Abdullah, and N. Q. A. AlShaikhli, "Inter-cell interference mitigation using adaptive reduced power subframes in heterogeneous networks", *International Journal of Electrical and Computer Engineering*, Vol. 11, No. 4, pp. 3275-3284, 2021.

[39] T. Rakia, H. C. Yang, M. S. Alouini, and F. Gebali, "Outage Analysis of Practical FSO/RF Hybrid System With Adaptive Combining", *IEEE Communications Letters*, Vol. 19, No. 8, pp. 1366-1369, 2015.

[40] H.-H. Lu *et al.*, "A combined fibre/free-space-optical communication system for long-haul wireline/wireless transmission at millimetre-wave/sub-THz frequencies", *Communications Engineering*, Vol. 2, No. 1, p. 18, 2023.

[41] S. Sharma, A. S. Madhukumar, and R. Swaminathan, "Switching-based hybrid FSO/RF transmission for DF relaying system", In: *Proc. of IEEE Wireless Communications and Networking Conference, WCNC*, Barcelona, Spain,Vol. 2018-April, pp. 1-6, 2018.

[42] K. O. Odeyemi and P. A. Owolawi, "Partial relay selection in mixed RF/FSO dual-hop system over unified M-distributed fading channel with non-zero boresight pointing errors", *Optical and Quantum Electronics*, Vol. 51, No. 5, 2019.

[43] R. Rani, A. Tiwari, A. Tiwari, A. Singh, A. Singh, and M. Lakshmanan, "Outage Performance of Hybrid FSO/RF-FSO Communication System with single threshold", In: *Proc. of 2023 2nd International Conference on Vision Towards Emerging Trends in Communication and Networking Technologies (ViTECoN)*, Vellore, India, pp. 1-5, 2023.

[44] S. Ghoname, H. A. Fayed, A. A. El Aziz, and M. H. Aly, "Performance evaluation of an adaptive hybrid FSO/RF communication system: impact of weather attenuation", *Iranian Journal of Science and Technology, Transactions of Electrical Engineering*, Vol. 44, pp. 119-128, 2020.

Received: June 17, 2024. Revised: July 26, 2024.

[45] V.-D. Phan *et al.*, "Performance of cooperative communication system with multiple reconfigurable intelligent surfaces over Nakagami-m fading channels", *IEEE Access*, Vol. 10, pp. 9806-9816, 2022.
[46] Y. Wu, D. Kong, Q. Wang, and G. Li, "Performance Analysis of UAV-Assisted Hybrid FSO/RF Communication Systems under Various Weather Conditions", *Sensors*, Vol. 23, No. 17, p. 7638, 2023.
[47] W. M. R. Shakir, "Performance analysis of the hybrid MMW RF/FSO transmission system", *Wireless Personal Communications*, Vol. 109, No. 4, pp. 2199-2211, 2019.